Efficient Conjugated-Polymer Optoelectronic Devices Fabricated by Thin-Film Transfer-Printing Technique

ARTICLE *in* ADVANCED FUNCTIONAL MATERIALS · APRIL 2008

Impact Factor: 11.81 · DOI: 10.1002/adfm.200701321

6 AUTHORS, INCLUDING:

Zijian Zheng
The Hong Kong Polytechnic University
67 PUBLICATIONS **1,774** CITATIONS
SEE PROFILE

Wilhelm Huck
Radboud University Nijmegen
250 PUBLICATIONS **13,515** CITATIONS
SEE PROFILE

FULL PAPER

ADVANCED FUNCTIONAL MATERIALS

DOI: 10.1002/adfm.200701321

Efficient Conjugated-Polymer Optoelectronic Devices Fabricated by Thin-Film Transfer-Printing Technique**

By *Keng-Hoong Yim, Zijian Zheng, Ziqi Liang, Richard H. Friend, Wilhelm T. S. Huck,** and *Ji-Seon Kim**

The fabrication of functional multilayered conjugated-polymer structures with well-defined organic-organic interfaces for optoelectronic-device applications is constrained by the common solubility of many polymers in most organic solvents. Here, we report a simple, low-cost, large-area transfer-printing technique for the deposition and patterning of conjugated-polymer thin films. This method utilises a planar poly(dimethylsiloxane) (PDMS) stamp, along with a water-soluble sacrificial layer, to pick up an organic thin film (~20 nm to 1 μm) from a substrate and subsequently deliver this film to a target substrate. We demonstrate the versatility of this transfer-printing technique and its applicability to optoelectronic devices by fabricating bilayer structures of poly(9,9-di-*n*-octylfluorene-*alt*-(1,4-phenylene-((4-*sec*-butylphenyl)imino)-1,4-phenylene))/poly(9,9-di-*n*-octylfluorene-*alt*-benzothiadiazole) (TFB/F8BT) and poly(3-hexylthiophene)/methanofullerene([6,6]-phenyl C_{61} butyric acid methyl ester) (P3HT/PCBM), and incorporating them into light-emitting diodes (LEDs) and photovoltaic (PV) cells, respectively. For both types of device, bilayer devices fabricated with this transfer-printing technique show equal, if not superior, performance to either blend devices or bilayer devices fabricated by other techniques. This indicates well-controlled organic-organic interfaces achieved by the transfer-printing technique. Furthermore, this transfer-printing technique allows us to study the nature of the excited states and the transport of charge carriers across well-defined organic interfaces, which are of great importance to organic electronics.

1. Introduction

There is increasing interest in electronically-functional organic materials for various applications. Conjugated polymers with semiconducting properties have been intensively investigated in the past decade for applications in optoelectronic devices such as light-emitting diodes (LEDs),[1,2] photovoltaic (PV) cells,[3,4] and field-effect transistors.[5,6] The possibility of tuning the optical and electronic properties by simply mixing materials with different properties is a strong merit of organic materials over inorganic crystalline materials such as silicon.

As the requirement for device performance increases, there is a greater demand for combining the functionalities of different organic materials into various device architectures. For solution-processed conjugated polymers, blending is a common strategy where two or more dissimilar polymers are mixed from a common organic solvent to achieve specifically-desired properties in the solid state without the need to synthesize new polymers.[7] For example, the use of conjugated-polymer blends as the active materials in LEDs and PV cells has been successful in enhancing device efficiency.[8–12] LEDs fabricated with poly(9,9-di-*n*-octylfluorene-*alt*-benzothiadiazole) (F8BT) blended with poly(9,9-di-*n*-octylfluorene-*alt*-(1,4-phenylene-((4-*sec*-butylphenyl)imino)-1,4-phenylene)) (TFB) as the emissive layer show a significantly-improved device performance, with an electroluminescence efficiency above 18 lm W^{-1} and excellent stability under prolonged operation (more than 5000 h at 100 cd m^{-2}).[8,9] One of the most-promising organic PV devices to date is based on the combination of poly(3-hexylthiophene) (P3HT) as a donor and methanofullerene([6,6]-phenyl C_{61} butyric acid methyl ester) (PCBM) as an acceptor, where an external quantum efficiency above 80% and a power

[*] Prof. W. T. S. Huck, Z. Zheng, Dr. Z. Liang
Melville Laboratory for Polymer Synthesis
Department of Chemistry
University of Cambridge
Lensfield Road, Cambridge CB2 1EW (UK)
E-mail: wtsh2@cam.ac.uk

Prof. W. T. S. Huck, Z. Zheng, Dr. Z. Liang
The Nanoscience Centre, University of Cambridge
J. J. Thomson Avenue, Cambridge CB3 0FF (UK)
E-mail: wtsh2@cam.ac.uk

Dr. J.-S. Kim
Blackett Laboratory, Imperial College London
Prince Consort Road, London SW7 2BW (UK)
E-mail: jkim1@imperial.ac.uk

Dr. J.-S. Kim, K.-H. Yim, Prof. R. H. Friend
Cavendish Laboratory, University of Cambridge
J. J. Thomson Avenue, Cambridge CB3 0HE (UK)

[**] The authors would like to thank Cambridge Display Technology (CDT) Ltd. for supplying the F8BT, TFB and P3HT materials and financial support (K.H.Y., Z.Z.), and Dr. P. Ho for the cross-linker. This work was funded by EPSRC (Dorothy Hodgkin Postgraduate Studentship (Z.Z.), Advanced Research Fellowship (J.-S.K.) and grants GR/S99075/1 and EP/C015401/1). K.H.Y., Z.Z., and Z.L. contributed equally to this work.

ADVANCED FUNCTIONAL MATERIALS

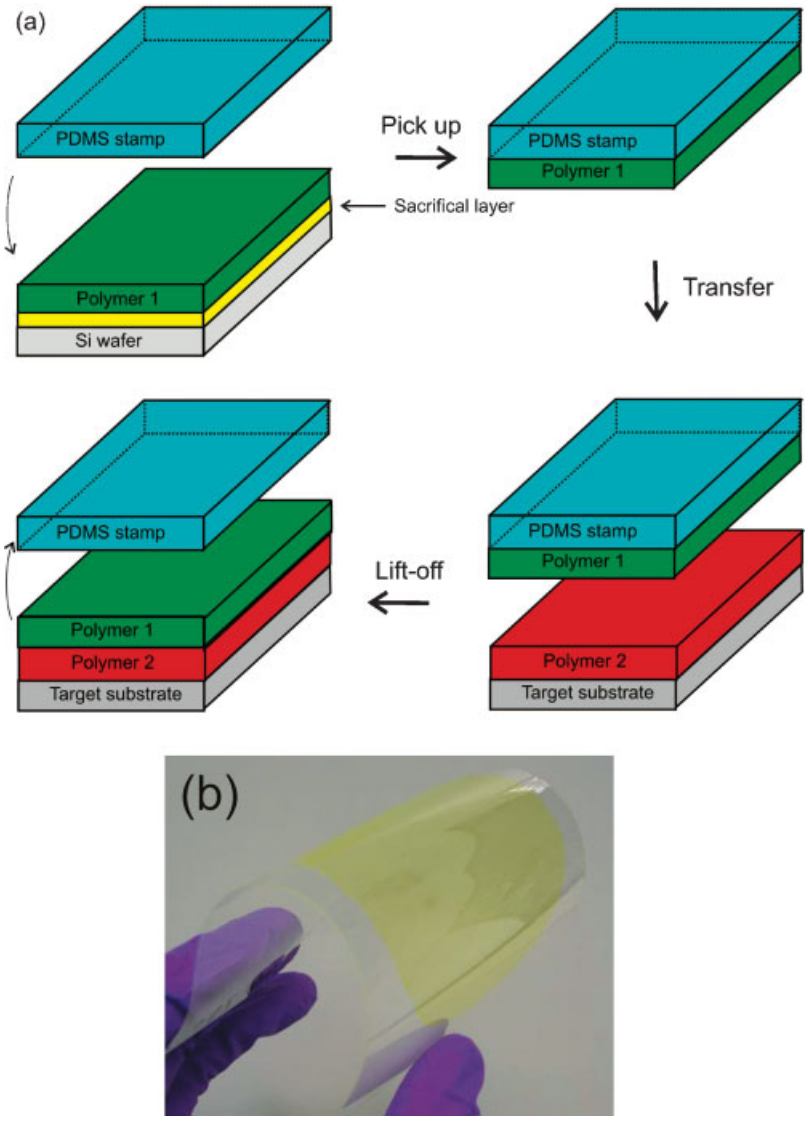

Figure 1. a) Schematic depiction of the thin-film transfer-printing process to form a bilayer conjugated-polymer structure. b) A photograph of a four-inch transfer-printed F8BT thin film (~70 nm) on a flexible PET sheet.

conversion efficiency approaching 5% have been reported recently.[11,12] However, due to the intrinsic immiscibility of most dissimilar conjugated-polymer mixtures, phase separation typically occurs in the polymer-blend thin film, creating 'distributed' organic-organic interfaces.[7] It is often difficult to precisely control the direction and length scale of such phase-separated structures, thereby limiting the variety of materials, and hence the electronic functionality in a blend film.

In contrast, co-sublimation (similar to blending for conjugated polymers) and successive sublimation of two or more different materials under vacuum are commonly used for small-molecule organic materials to form functional multilayered structures.[13–15] For instance, highly-efficient small-molecule organic LEDs typically consist of well-defined hole- and electron-transporting layers and different emissive layers.[14,15] The ability to fabricate such multilayered structures is of critical importance for device optimization, because one can then control precisely the distance of the charge-recombination zone (for LEDs) or the charge-generation zone (for PV cells) from the electrodes.

In order to overcome difficulties for the fabrication of such multilayered structures in solution-processed conjugated polymers, a variety of lamination and transfer-printing techniques that have been developed recently for the deposition of metal electrodes and organic layers could allow for greater manufacturability of organic electronic devices with low cost and at high processing speed. These dry-transfer methods can be organized into (i) metal transfer onto metals and organics;[16–22] and (ii) transfer of organics onto metals and organics.[23–27] To achieve multilayered conjugated-polymer structures, common strategies involve complex cross-linking and polymer synthetic routes to ensure that the solvent used for the subsequent layers is resistant to the preceding layer.[28–31] However, such methods are applicable to only a limited combination of materials as cross-linkers have to be chosen such that the effects on the electronic functionalities of the cross-linked materials are minimal. Transfer printing would eliminate the solvent-compatibility issues, but has to date only been used to transfer print electrodes or to laminate the final devices. There are no reports on transfer printing to fabricate multilayer organic electronic devices, which would give full control over the chemical composition and thickness of each layer, and it is precisely this area of application we would like to address in this work.

Herein we report a simple and general transfer-printing methodology for the fabrication of multilayered conjugated-polymer structures. This method is applicable on various inorganic and organic substrates over a large area. It involves a combined exploitation of an elastomeric poly(dimethylsiloxane) (PDMS) stamp as a scaffold for the transfer of donor organic films onto a range of receiving substrates, and a sacrificial layer, in contrast to the more-frequently-reported self-assembled monolayer-based adhesion-enhancement (on the acceptor substrate) or reduction (on the donor substrate) layers, as a removable intermediate. In our hands, a polymeric sacrificial layer resulted in significantly-more-reliable and reproducible transfer printing. By employing the soft, adhesive nature of PDMS to grab the solid objects from one surface and release them onto another, the large-scale integration of functional objects of a variety of sizes and shapes into spatially-organized systems is possible,

while totally eliminating the issue of organic-solvent compatibility when generating organic multilayer structures. Notably, this transfer-printing process does not involve plasma oxidation, high-pressure and/or high-temperature annealing, thereby avoiding possible degradation of the organic thin films. As a proof-of-concept, we demonstrate the use of this transfer-printing technique to form bilayer polymer structures for LED and PV cell applications.

2. Results

The schematic drawing in Figure 1a describes a typical transfer-printing procedure. A flat PDMS stamp is first pressed into conformal contact on the donor thin film deposited on a water-soluble sacrificial layer such as poly(sodium 4-styrene sulfonate) (PSSNa). The PSSNa layer and donor thin film were sequentially spin-coated onto an oxygen-plasma-treated Si wafer from aqueous solution and organic solvent, respectively. The sacrificial layer was removed by placing the sample together with the PDMS stamp into a water bath and, as a result, the film of interest was transferred onto the PDMS stamp. Subsequently, the donor-film-inked PDMS stamp was placed onto the receiving substrate and deposited upon delamination of the PDMS stamp. The solid-state transfer process is mainly governed by the difference between the adhesion strength of the two contact surfaces (the PDMS-organic and organic-substrate interfaces). Once the wetting due to the conformal contact is formed, the film on the PDMS stamp of low surface tension is readily transferred onto various flat substrates with a higher surface energy. We note that this transfer-printing process is, in accordance with work by Rogers et al.,[32,33] kinetically favorable and largely influenced by the physics of soft adhesion that, in turn, strongly depends on the rate at which solid objects are transferred to and from an elastomeric stamp. Depending on the surface properties of the receiving substrate, moderate thermal treatment might be required during the delamination process to increase the work adhesion between the donor film and the receiving substrate. We have successfully applied this transfer-printing technique to a variety of conjugated polymers, with film thicknesses varying from 20 nm to 1 μm, onto a range of different substrates including Si wafers, quartz and indium tin oxide (ITO)-coated glass substrates, as well as flexible poly(ethylene terephthalate) (PET) sheets, some of which were pre-coated with organic thin films. Figure 1b displays a photograph of a four-inch yellow-green-emitting F8BT thin film (~80 nm) that was transfer printed onto a flexible PET sheet. All of these laminated films cannot be simply removed from the substrates by using a Scotch tape. Repeating the lamination/delamination steps described above yields the formation of multilayered conjugated-polymer structures (not shown). The PDMS stamp can be reused for lamination more than 10 times without any obvious influence on the quality of the printed thin films. Transfer printing much thinner films is currently limited by the mediocre quality of spun-cast films with thicknesses $\ll$20 nm. We will report on the transfer printing of patterned films using either patterned PDMS stamps or pre-patterned polymer films in the future.

In order to investigate the possible degradation of the optical properties of the F8BT ($M_n = 9$ kg mol^{-1}) thin film caused by the transfer-printing process we measured the photoluminescence (PL) efficiency both in the pristine and annealed states. For a pristine F8BT thin film (~80 nm), the PL efficiency decreased slightly from 65% to 60% after the transfer-printing process. This reduction might be due to the residual sacrificial layer (PSSNa) left on the transfer-printed film that acts as a luminescence-quenching site. However, upon annealing above the glass-transition temperature ($T_g = 160\,^{\circ}$C) under nitrogen after the transfer-printing process, the PL efficiency recovered to 75%, similar to that of an annealed spin-coated F8BT film.[34] The increase in PL efficiency upon annealing above T_g is understood by considering the restructuring of the F8BT chains to adopt a local configuration that hinders interchain exciton migration to the less- or non-emissive low-energy sites, thereby reducing the chances of luminescence quenching. Hence we have shown that the transfer-printing process has only a very limited effect on the luminescence properties of conjugated polymers.

The lamination-transfer method affords a high degree of control over the interface quality under ambient laboratory conditions, thus giving rise to smooth interfacial contacts between the two laminated parts. The expected low electrical interfacial resistivity offers opportunities for fabricating high-performance polymer electronic devices based on multilayered structures, which are not normally achievable for solution-processed polymers. To examine the utility of this transfer-printing technique, we fabricated LEDs and PV cells with appropriate bilayer polymer structures as the active materials.

For LEDs, we chose to work with the TFB and F8BT system as these polyfluorene derivatives are highly efficient and relatively well-studied in the literature.[9,10,30,35] The chemical structures of these materials are shown in Figure 2a. We incorporated the bilayer structure of TFB (20 nm, spin-coated)/F8BT (80 nm, transfer printed) as active layers into a standard LED architecture. We note that thermal annealing of the bilayer structure (above T_g of the transfer-printed film) in a nitrogen environment helps to improve the adhesion between the organic layers, and hence reduces the interfacial electrical resistivity. For comparison, we also fabricated an identical bilayer structure using a UV cross-linker to cross-link the underlying TFB layer (20 nm) prior to spin-coating of the F8BT layer (80 nm), as described elsewhere.[30,31]

Figure 2b compares the electroluminescence (EL) efficiency of the corresponding LEDs. All the devices exhibit sharp turn-on in both current and luminance at ~2 V. Typically, F8BT:TFB blend films from *xylene* solution exhibit micron-scale lateral phase separation as shown in the inset of Figure 2c.[35] Such characteristic morphology assists in achieving high initial EL efficiency due to confined charge-carrier recombination at the polymer-polymer interfaces. However, the rough-blend film surface with very-thin TFB-rich domains

ADVANCED FUNCTIONAL MATERIALS

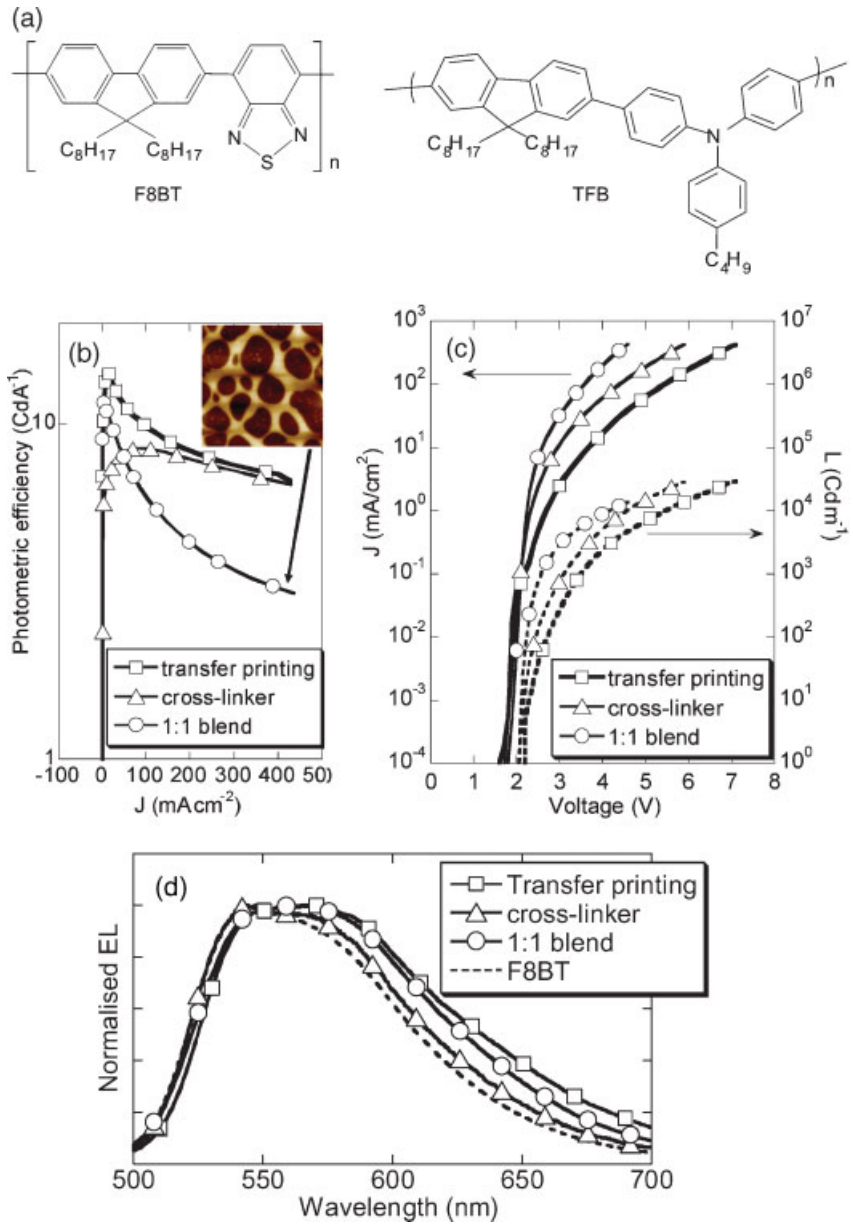

Figure 2. a) Chemical structures of F8BT and TFB materials. b) Electroluminescence efficiency (Cd A^{-1}) as a function of diode current (*J*) of LEDs with TFB/F8BT bilayer films (20nm/80nm) fabricated by the transfer-printing technique (square) and with a cross-linker (triangles), and the TFB:F8BT blend film (1:1 by weight, circle). The AFM image (20 μm × 20 μm, 70 nm height scale) of the blend film is included in the inset, showing a micron-scale lateral phase separation with characteristic TFB-rich islands embedded in F8BT-rich matrices. c) Current-voltage-luminance (*J-V-L*) characteristics and d) normalized EL spectra of the same set of devices. An EL spectrum of a pristine F8BT device is included for comparison.

causes the leakage current to increase at high voltages, as more holes arrive at the cathode without undergoing radiative recombination with electrons.[35] For example, the EL efficiency of the blend device drops by almost an order of magnitude from 11 Cd A^{-1} at 2.3 V to 3 Cd A^{-1} at 4.6 V. On the other hand, bilayer TFB/F8BT devices overcome the shortfall of such blend devices with a uniform film surface and a well-defined polymer-polymer interface as the electron-hole recombination zone. As shown in Figure 2b, the transfer-printed bilayer TFB/F8BT device shows an improved EL efficiency compared to the blend device, achieving 14 Cd A^{-1} at 3.8 V and 7 Cd A^{-1} at 7 V. Similarly, the identical bilayer TFB/F8BT device fabricated with cross-linkers shows comparable EL performance, also with a slower decay of the EL efficiency at high voltages. The general trend of EL efficiency for bilayer devices observed here is in good agreement with similar bilayer structures in the literature, formed using interlayer, float-off and inkjet-printing techniques.[36–39] This demonstrates that the transfer-printing technique is applicable for fabricating multilayered conjugated-polymer structures for functional LEDs without significant degradation to their optical and electronic properties. Overall, the EL efficiency for transfer-printed bilayer TFB/F8BT device is higher than that of a blend device at all levels of current densities (Fig. 2b). We attribute this improvement to reduced exciton quenching, taking place at the well-defined polymer-polymer heterojunction in the bilayer structure, than in the blend film that has higher density of 'distributed' polymer-polymer interfaces. As expected, the PL efficiency of the transfer-printed TFB/F8BT bilayer structure is 70% (85% for the pristine F8BT film), which is 40% for the blend film. In principle, the EL efficiency of the bilayer device can be further optimized by shifting the well-defined electron-hole recombination zone (polymer-polymer interface) away from the electrodes (which are known to quench the luminescence),[36,40,41] while optimizing the optical-cavity effect within the active layers. This optimization can be achieved by changing the relative thickness of the individual polymer films in the bilayer structure, taking into account energy levels and carrier mobilities of these materials. Such precise engineering of polymer-polymer interfaces for the device application is not easily achievable by blending and spin-coating.

Figure 2c shows the luminance-voltage and current-voltage characteristics of these devices, with an F8BT:TFB-blend (1:1

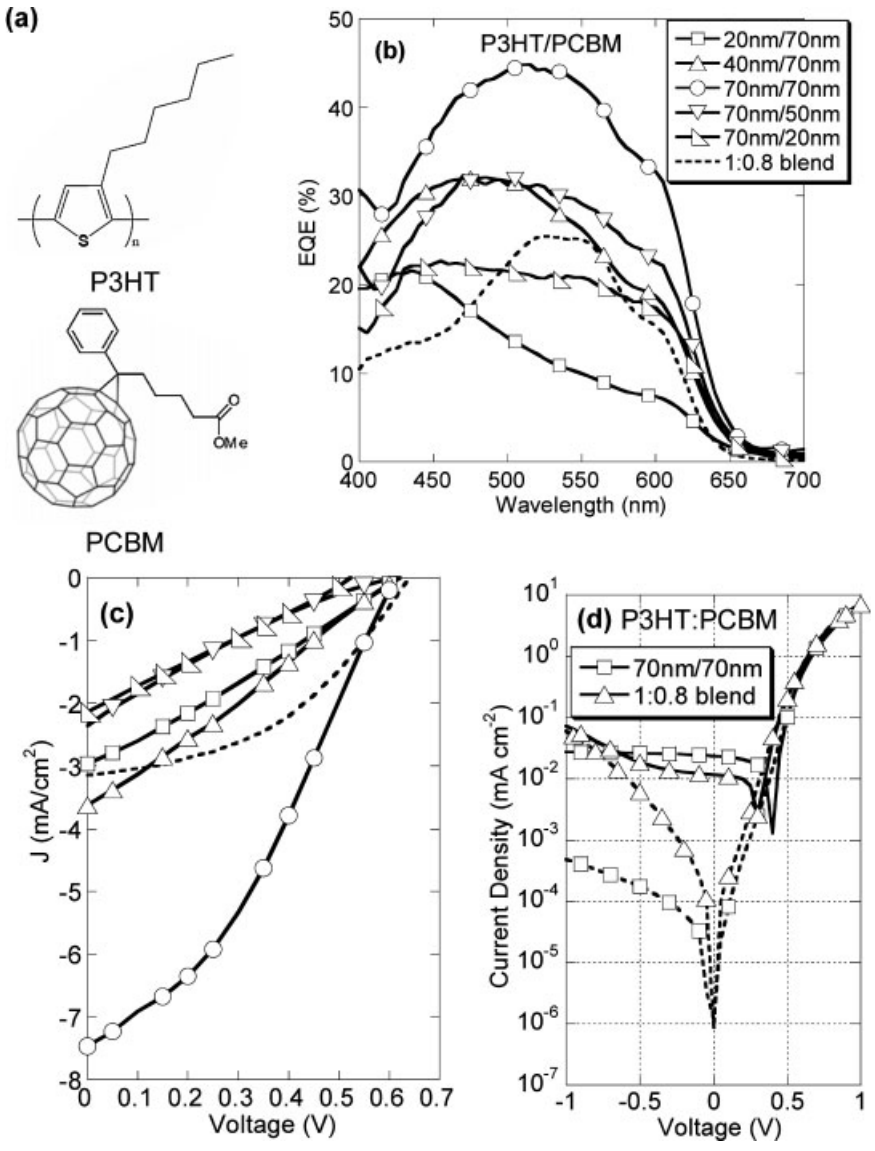

Figure 3. a) Chemical structures of P3HT and PCBM materials. b) External quantum efficiency (EQE) of P3HT/PCBM bilayered solar cells fabricated by transfer printing technique, with different thicknesses of either P3HT or PCBM (20–70 nm), while keeping the thickness of the other material (70 nm) and other processing conditions constant. An EQE spectrum of a P3HT:PCBM blend device (1:0.8 by weight) is included for comparison. c) Current-voltage characteristics of the same set of devices under AM1.5 illumination at 100 mW/cm^2. d) Current-voltage characteristics of a transfer-printed P3HT/PCBM bilayered device (70 nm/70 nm) and a blend device in the dark (dashed lines) and under low intensity (~1 mW/cm^2) illumination at 550 nm (solid lines).

by weight) device as a reference. At a fixed voltage, the current and luminance of the transfer-printed bilayer device are slightly lower than other devices, which can be attributed to interfacial electrical resistance within the bilayer structure.

Figure 2d shows normalized EL spectra of the devices studied. Compared to the single-layer F8BT device, both the bilayer and blend devices, albeit to a different extent, show red-shifted EL spectra, which we assign to the formation of an interface state (termed ''exciplex'') at F8BT:TFB heterojunctions.[9,30] The formation of such an interface state is found to be dependent sensitively on the relative local arrangement of the polymer chains at the interfaces, on the molecular scale. This explains the subtle differences in the EL spectra between the bilayer device fabricated by the transfer-printing technique and cross-linkers, although these devices are very similar in terms of device layout.

For PV applications, we studied the performance of devices based on bilayer heterojunctions of P3HT and PCBM, whose chemical structures are shown in Figure 3a. Bulk heterojunction PV devices fabricated from blends of P3HT and PCBM have been extensively studied showing several breakthroughs in efficiency, as a result of efficient photoinduced electron transfer from conjugated polymers to fullerene molecules.[12,13,42] It is known that the thickness of the active layer in a PV cell has significant influence on the short-circuit spectra and efficiency,[43–45] as it influences processes fundamental to

ADVANCED FUNCTIONAL MATERIALS

the device operation, namely charge-carrier transport and photogeneration of excitons and resulting free charge carriers. The spatial distribution of light intensity within the device structure is periodically modulated due to optical interference between the incident and back-reflected light. For blend systems, investigation of these effects on the device operation by varying the film thickness is not straight forward, as the phase-separation process is typically strongly dependent on film thickness, which influences the compositions of the phase-separated domains (for charge transport) and distribution of heterojunction sites (for photogeneration). In contrast, bilayer structures with well-controlled organic-organic interfaces fabricated by the transfer-printing technique could eliminate these shortcomings.

To investigate the effects on the short-circuit photocurrent spectra and efficiency, we systematically varied the thickness of one of the layers from 20 nm to 70 nm while keeping the other film constant at 70 nm. In this bilayer structure, the PCBM layer functions as an electron-transporting layer, whereas the P3HT layer is responsible for light absorption and hole transport. Since the intensity of light is low near the metallic electrode due to the optical-interference effect, the photogeneration of free charge carriers is significantly reduced in this dead zone. Considering the relatively-high electron mobility of PCBM (2×10^{-3} cm^2 V^{-1} s^{-1})[42], it could be used as a buffer layer, along with changing the P3HT film thickness to tune the optical cavity in the active layer such that the exciton dissociation zone (within ~10–15 nm from P3HT/PCBM interface) falls within the maximum light absorption zone.[13,43]

Figure 3b shows the external quantum efficiency (EQE) of P3HT/PCBM bilayer devices with different thicknesses of both layers, fabricated by the transfer-printing technique, under a low incident monochromatic light intensity (~1 mW cm^{-2}). The performance of a blend device (P3HT:PCBM = 1:0.8 by weight) is included as a reference. Figure 3c shows the corresponding current-voltage characteristics of the same set of devices under *Air Mass* 1.5 (AM 1.5) illumination at 100 mW cm^{-2}. We note that the performance of the blend device (peak EQE ~25%, power efficiency 0.9%) is poorer than that found in the literature (peak EQE ~60%, power efficiency ~2–3%).[13] This might be due to a different quality of P3HT, handling of polymer solutions and thin films in air, as well as other non-optimized processing conditions. When repeated in a nitrogen environment, the blend device shows a significantly-improved performance, with a peak EQE of ~32% and a power efficiency of ~1.7%. Hence the performance of PV cells reported here sets the lowest limit and could be potentially improved appreciably under optimized processing conditions. Nevertheless, the blend device (processed in air) should serve as a reasonable reference in our study to compare with the bilayer devices fabricated in air.

Firstly, there is no clear dependence of the open-circuit voltage (V_{OC}) of these devices on the active-layer thickness, as all of them show $V_{OC} \sim 0.5$–0.6 V. When the PCBM thickness was fixed at 70 nm, the maximum EQE was only ~23% for devices with a 20 nm thick P3HT layer. The peak position (435 nm) was blue shifted relative to the main absorption band of P3HT at ~520 nm. This is because most of the photocurrent contribution comes from the PCBM absorption shoulder at ~450 nm, which is non-optimized for PV cells considering the larger mismatch with the solar spectrum. As the P3HT thickness was gradually increased to 40 nm and 70 nm, the short-circuit photocurrent spectrum approached the absorption spectrum of P3HT, and the maximum EQE increased to 32% and 45%, respectively. Under AM 1.5 illumination, the short-circuit current of these devices also increased from 3.1 mA cm^{-2} to 3.8 mA cm^{-2} then 7.6 mA cm^{-2} with increasing P3HT film thickness (Fig. 3c), as expected from the EQE spectra. The maximum power-conversion efficiency of 1.7% with a fill factor of ~40% was achieved for the 70 nm/70 nm bilayer device.

When the thickness of P3HT layer was kept constant at 70 nm, the EQE gradually dropped to 32% and 23% with decreasing PCBM film thickness. The photocurrent-action spectra show only slight blue shifts with respect to the absorption band of P3HT, indicating that the main contribution to photocurrent comes from the P3HT layer, rather than the PCBM layer that is directly next to the metal electrode. Considering that the light intensity is virtually zero near the aluminum electrode, we attribute the decrease of EQE to reduced photogeneration of charge carriers, as the distance between the polymer-polymer heterojunction (charge dissociation zone) and electrode decreases with decreasing PCBM thickness. Under AM 1.5 illumination (Fig. 3c), the short-circuit current rapidly dropped to 2.7 mA cm^{-2} and 2.4 mA cm^{-2} when the PCBM thickness was reduced to 50 nm and 20 nm, respectively. We consider the imbalance of charge-carrier mobilities in the P3HT and PCBM layers important for such a rapid decrease in the short-circuit current under high-intensity illumination (~100 mW cm^{-2}).

The observed changes of the photocurrent-action spectra and efficiency as a function of film thickness is in agreement with the literature, where bilayer structures were formed by solution processed conjugated polymers along with an evaporated fullerene (C_{60}) layer.[45] This example shows that with well-defined polymer-polymer interfaces in the bilayer structures studied here, we could vary the exciton dissociation zone, thereby allowing the study (and verification) of the device physics. We believe further optimization of the device performance is possible, taking into account the optical-interference effect and the charge-carrier transport properties of the active layers.

Figure 3d compares the current-voltage characteristics of the P3HT:PCBM blend device and a bilayer device (70 nm/70 nm), both in the dark and under low incident-light intensity (~1 mW cm^{-2}) at 550 nm. We observed that the bilayer device shows much higher rectifying behaviour in the dark than the blend device. The dark current of the bilayer device under reverse electric field is significantly lower than that of the blend device. We attributed this to higher shunt resistance of bilayer devices compared to that of blend devices, due to the lack of a continuous pathway of either

polymer in the active layer to both electrodes. Such a characteristic is generic to all of the bilayer devices studied here and agrees well with the literature.[45] Bilayer devices fabricated by this transfer-printing technique may find applications in organic photodetectors where there is a need to suppress the dark current to obtain a high light/dark-current contrast (ON/OFF ratio).[46]

3. Conclusion

We have demonstrated a cost-effective yet viable transfer-printing approach to the deposition and patterning of uniform active conjugated-polymer thin films for organic electronic device applications. A planar PDMS stamp is utilized along with a sacrificial layer for picking up solid-state organic thin films from substrates and subsequently delivering them to target substrates. The transfer-printed thin films (down to ~20 nm thick) reveal a remarkably smooth surface and are pinhole-free. Our approach has clearly manifested its simplicity for dry transfer, additivity of depositing successive layers, and versatility of application to different functional materials. To evaluate the applicability of this technique to conjugated-polymer-based optoelectronic devices, we fabricated bilayer LEDs based on a TFB/F8BT system and PV cells based on a P3HT/PCBM system. In both cases, bilayer devices fabricated with this transfer-printing technique show an equal, if not superior performance, to either blend devices or bilayer devices fabricated by other techniques. More importantly, this transfer-printing technique provides a powerful tool for systematically and easily manipulating organic-organic interfaces, which facilitates the study of polymer-heterojunction photophysics, and understanding of device physics. This transfer-printing technique can, in principle, be repeated multiple times to fabricate multilayered conjugated-polymer structures that provide opportunities for new device architectures and applications. It holds great promise for low-cost, large-area and high-throughput fabrication of diverse organic electronic devices, while allowing us to carry out fundamental studies on interfacial charge transport of organic electronics in a precisely controlled manner.

4. Experimental

F8BT ($M_n = 255\,kg\,mol^{-1}$, unless otherwise stated) and TFB ($M_n = 106\,kg\,mol^{-1}$) were received from Cambridge Display Technology (CDT) Ltd. P3HT was purchased from Sigma-Aldrich and purified by CDT before use. PCBM was purchased from Nano-C Inc.

All of the polymer solutions were prepared in air by dissolving each polymer in either *p*-xylene (F8BT and TFB) or chlorobenzene (P3HT and PCBM) to produce a concentration of 0.5–2.5% w/v, depending on the desired film thickness. For the F8BT:TFB blend, both solutions of the pristine polymers were mixed at a ratio of 1:1 by weight. For the P3HT:PCBM blend, P3HT (1% w/v) and PCBM (0.8% w/v) were mixed at a 1:1 volume ratio[12,13]. Polymer films between ~20 and 100 nm thick were then spin-coated in air from these solutions onto pre-cleaned quartz substrates (for optical measurements) or silicon substrates pre-coated with a water-soluble sacrificial layer of PSSNa, unless otherwise stated (for transfer printing).

The cross-linker used to fabricate bilayer the TFB/F8BT devices was ethylene bis(4-azido-2,3,5,6-tetrafluorobenzenesulfonamide). A spin-coated ~100 nm thick TFB layer with cross-linker (0.8% by weight) was exposed to UV radiation and subsequently spin-rinsed with solvent to produce a cross-linked layer approximately 20 nm thick, prior to the deposition of the F8BT layer. The cross-linking occurs via a non-specific nitrene insertion into the alkyl and aromatic C–H bonds and therefore does not affect the primary conjugation of the polymers. Detailed processing steps are discussed elsewhere[30,31].

LEDs were fabricated by using ITO as anode, the F8BT:TFB blend or bilayer film as the active layer, and Ca/Al as the cathode. A poly(styrene sulphonate)-doped poly(3,4-ethylene dioxythiophene) (PEDOT:PSS) layer approximately 60 nm thick was first spin-coated onto an oxygen-plasma-treated ITO-coated glass substrate and then baked at 200 °C for 1 h under N_2 flow, prior to the deposition of the polymer active layer. Finally, Ca (~20 nm) with an Al (~100 nm) protecting layer was thermally evaporated at a base pressure of $\sim 10^{-6}$ mbar. PV cells were fabricated in a similar way, except with a P3HT/PCBM bilayer or blend film as the active layer, and Al (~100 nm) as cathode. For both types of device, thermal annealing of the transfer-printed bilayer structures at 160 °C for 1 h in nitrogen environment was performed prior to cathode deposition to improve the adhesion between the organic layers and reduce the interfacial electrical resistivity. Post-evaporation thermal annealing of the P3HT:PCBM blend device was performed at 150 °C for 30 min in a nitrogen environment.

The PL spectra and efficiencies were measured at room temperature in an integrating sphere with excitation from an Ar ion laser at 355/365 nm for the F8BT and/or TFB films. The calculations for the PL efficiencies were described by de Mello et al.[47].

The current-voltage-luminance (*J-V-L*) characteristics of the LEDs were measured under vacuum ($\sim 10^{-1}$ mbar) by a computer-controlled HP 4145B semiconductor parameter analyzer, coupled to a calibrated silicon photodiode placed in the forward direction normal to the device substrate. The EL spectra were measured at the forward direction with a silica fiber bundle that was fed into a calibrated Oriel spectrometer.

For the PV cells, the current-voltage (*J-V*) curves were measured under nitrogen at room temperature using a Keithley 237 source-measure unit. The photocurrent spectra were recorded with illumination from a Xenon lamp dispersed through a single-grating monochromator. The current-voltage characteristics under AM 1.5 illumination (100 mW cm^{-2}) were measured using a solar simulator (Oriel Instruments 81160). The power efficiencies were corrected for spectral mismatch between the solar simulator and the true AM 1.5 spectrum.

Received: November 12, 2007
Revised: December 19, 2007
Published online: March 31, 2008

[1] R. H. Friend, R. W. Gymer, A. B. Holmes, J. H. Burroughes, R. N. Marks, C. Taliani, D. D. C. Bradley, D. A. Dos Santos, J. L. Brédas, M. Lögdlund, W. R. Salaneck, *Nature* **1999**, *397*, 121.

[2] P. K. H. Ho, J.-S. Kim, J. H. Burroughes, H. Becker, S. F. Li, T. M. Brown, F. Cacialli, R. H. Friend, *Nature* **2000**, *404*, 481.

[3] J. J. M. Halls, C. A. Walsh, N. C. Greenham, E. A. Marseglia, R. H. Friend, S. C. Moratti, A. B. Holmes, *Nature* **1995**, *376*, 498.

[4] A. C. Arias, N. Corcoran, M. Banach, R. H. Friend, W. T. S. Huck, *Appl. Phys. Lett.* **2002**, *80*, 1695.

[5] L. L. Chua, J. Zaumseil, J.-F. Chang, E. C. W. Ou, P. K. H. Ho, H. Sirringhaus, R. H. Friend, *Nature* **2005**, *434*, 194.

[6] H. Sirringhaus, P. J. Brown, R. H. Friend, M. M. Nielsen, K. Bechgaard, B. M. W. Langeveldvoss, A. J. H. Spiering, R. A. J. Janssen, E. W. Meijer, P. Herwig, D. M. Deleeuw, *Nature* **1999**, *401*, 685.
[7] E. Moons, *J. Phys. Condens. Matter* **2002**, *14*, 12235.
[8] A. C. Morteani, A. S. Dhoot, J.-S. Kim, C. Silva, N. C. Greenham, C. Murphy, E. Moons, S. Ciná, J. H. Burroughes, R. H. Friend, *Adv. Mater.* **2003**, *15*, 1708.
[9] J.-S. Kim, P. K. H. Ho, C. Murphy, N. Baynes, R. H. Friend, *Adv. Mater.* **2002**, *14*, 206.
[10] J. J. M. Halls, A. C. Arias, J. D. MacKenzie, W. Wu, M. Inbasekaran, E. P. Woo, R. H. Friend, *Adv. Mater.* **2000**, *12*, 498.
[11] W. Ma, C. Yang, X. Gong, K. Lee, A. J. Heeger, *Adv. Funct. Mater.* **2005**, *15*, 1617.
[12] J. Y. Kim, S. H. Kim, H.-H. Lee, K. Lee, W. Ma, X. Gong, A. J. Heeger, *Adv. Mater.* **2006**, *18*, 572.
[13] A. Yakimov, S. R. Forrest, *Appl. Phys. Lett.* **2002**, *80*, 1667.
[14] Y. Sun, N. C. Giebink, H. Kanno, B. Ma, M. E. Thompson, S. R. Forrest, *Nature* **2006**, *440*, 908.
[15] B. W. D'Andrade, J. Brooks, V. Adamovich, M. E. Thompson, S. R. Forrest, *Adv. Mater.* **2002**, *14*, 1032.
[16] C. Kim, P. E. Burrows, S. R. Forrest, *Science* **2000**, *288*, 831.
[17] Y.-L. Loo, R. L. Willett, K. W. Baldwin, J. A. Rogers, *Appl. Phys. Lett.* **2002**, *81*, 562.
[18] Y.-L. Loo, R. L. Willett, K. W. Baldwin, J. A. Rogers, *J. Am. Chem. Soc.* **2002**, *124*, 7654.
[19] E. Menard, L. Bilhaut, J. Zaumseil, J. A. Rogers, *Langmuir* **2004**, *20*, 6871.
[20] E. Menard, K. J. Lee, D. Y. Khang, R. G. Nuzzo, J. A. Rogers, *Appl. Phys. Lett.* **2004**, *84*, 5398.
[21] T.-W. Lee, J. Zaumseil, Z. Bao, J. W. P. Hsu, J. A. Rogers, *Proc. Natl. Acad. Sci, USA* **2004**, *101*, 429.
[22] D. A. Bernards, T. Biegala, Z. A. Samuels, J. D. Slinker, G. G. Malliaras, S. Flores-Torres, H. D. Abruña, J. A. Rogers, *Appl. Phys. Lett.* **2004**, *84*, 3675.
[23] T.-F. Guo, S. Pyo, S.-C. Chang, Y. Yang, *Adv. Funct. Mater.* **2001**, *11*, 339.
[24] M. Ofuji, A. J. Lovinger, C. Kloc, T. Siegrist, A. J. Maliakal, H. E. Katz, *Chem. Mater.* **2005**, *17*, 5748.
[25] M. L. Chabinyc, A. Salleo, Y. Wu, P. Liu, B. S. Ong, M. Heeney, I. McCulloch, *J. Am. Chem. Soc.* **2004**, *126*, 13928.
[26] A. L. Briseno, M. Roberts, M.-M. Ling, H. Moon, E. J. Nemanick, Z. Bao, *J. Am. Chem. Soc.* **2006**, *128*, 3880.
[27] Z. Zheng, O. Azzaroni, F. Zhou, W. T. S. Huck, *J. Am. Chem. Soc.* **2006**, *128*, 7730.
[28] X. Gong, S. Wang, D. Moses, G. C. Bazan, A. J. Heeger, *Adv. Mater.* **2005**, *17*, 2053.
[29] Y.-H. Niu, M. S. Liu, J.-W. Ka, J. Bardeker, M. T. Zin, R. Schofield, Y. Chi, A. K.-Y. Jen, *Adv. Mater.* **2007**, *19*, 300.
[30] A. C. Morteani, P. K. H. Ho, R. H. Friend, C. Silva, *Appl. Phys. Lett.* **2005**, *86*, 163501.
[31] S.-H. Khong, S. Sivaramakrishnan, R.-Q. Png, L.-Y. Wong, P.-J. Chia, L.-L. Chua, P. K. H. Ho, *Adv. Funct. Mater.* **2007**, *17*, 2490.
[32] S.-H. Hur, D.-Y. Khang, C. Kocabas, J. A. Rogers, *Appl. Phys. Lett.* **2004**, *85*, 5730.
[33] M. A. Meitl, Z.-T. Zhu, V. Kumar, K. J. Lee, X. Feng, Y. Y. Huang, I. Adesida, R. G. Nuzzo, J. A. Rogers, *Nat. Mater.* **2006**, *5*, 33.
[34] C. L. Donley, J. Zaumseil, J. W. Andreasen, M. M. Nielsen, H. Sirringhaus, R. H. Friend, J.-S. Kim, *J. Am. Chem. Soc.* **2005**, *127*, 12890.
[35] J.-S. Kim, P. K. H. Ho, C. E. Murphy, R. H. Friend, *Macromolecules* **2004**, *37*, 2861.
[36] J.-S. Kim, R. H. Friend, I. Grizzi, J. H. Burroughes, *Appl. Phys. Lett.* **2005**, *87*, 023506.
[37] Y. Xia, R. H. Friend, *Adv. Mater.* **2006**, *18*, 1371.
[38] Y. Xia, R. H. Friend, *Macromolecules* **2005**, *38*, 6466.
[39] Y. Xia, R. H. Friend, *Appl. Phys. Lett.* **2006**, *88*, 163508.
[40] K. H. Yim, R. H. Friend, J.-S. Kim, *J. Chem. Phys.* **2006**, *124*, 184706.
[41] F. Cacialli, S. E. Burns, H. Becker, *Opt. Mater.* **1998**, *9*, 168.
[42] P. W. M. Blom, V. D. Mihailetchi, L. J. A. Koster, D. E. Markov, *Adv. Mater.* **2007**, *19*, 1551.
[43] L. A. A. Pettersson, L. S. Roman, O. Inganas, *J. Appl. Phys.* **1999**, *86*, 487.
[44] A. J. Moulé, J. B. Bonekamp, K. Meerholz, *J. Appl. Phys.* **2006**, *100*, 094503.
[45] T. Stubinger, W. Brutting, *J. Appl. Phys.* **2001**, *90*, 3632.
[46] P. Peumans, V. Bulovic, S. R. Forrest, *Appl. Phys. Lett.* **2000**, *76*, 3855.
[47] J. C. de Mello, H. F. Wittmann, R. H. Friend, *Adv. Mater.* **1997**, *9*, 230.